

Lineament Fabric from Airborne LiDAR and its Influence on Triggered Earthquakes in the Koyna-Warna Region, Western India

Kusumita Arora^{1*}, R. K. Chadha¹, Y. Srinu¹, Adrien Selles², Srinagesh Davuluri¹, Vladimir Smirnov³, Alexander Ponomarev³ and V. O. Mikhailov³

¹ CSIR-National Geophysical Research Institute, Hyderabad - 500 007, India

² BRGM, D3E/NRE Unit, Indo-French Centre for Groundwater Research, CSIR-NGRI, Hyderabad - 500 007, India

³ Schmidt Institute of the Physics of the Earth RAS, Moscow, Russia

*E-mail: karora_ngri@yahoo.co.uk

ABSTRACT

We present the results of the first airborne LiDAR survey flown in the Koyna-Warna region and examine the relationship between the lineament fabric and the ongoing seismicity in the region. Our studies reveal that earthquakes of $M \geq 4.0$ for the period 1968 to 2016 are strongly correlated with a 10 km wide N-S fracture zone, which not only represents the surface expression of seismically active basement faults, but also act as conduits for water percolation between the Koyna and Warna reservoirs. A decreasing trend in the annual distribution of earthquakes was observed from 1985. A new burst of seismic activity in 1993 followed the impoundment of the Warna reservoir. We report a change in annual seismicity pattern, where seismicity peaks during September and December in the pre-Warna period, with a new peak emerging during March-April subsequent to the impoundment of Warna reservoir. A model is proposed to explain the seismicity along dominant N-S lineaments and the impact of Warna reservoir impounding which altered the hydrogeologic regime in the region.

INTRODUCTION

The Koyna Warna Seismic Zone (KWSZ) in western India is the locale of world's largest known triggered earthquake of $M 6.3$ in 1967 (Fig.1). The seismicity in the region has been found to be related to loading and unloading cycles of Koyna and Warna reservoirs (Gupta, 1992, 2002, 2005; Rastogi et al., 1997; Pandey and Chadha, 2003). Both these reservoirs lie on an elevated north-south (N-S) escarpment parallel to the west coast of India which is considered to be faulted (Pascoe, 1964; Valdiya, 1984). The region is underlain by the Deccan Traps of 67.4 Ma (Duncan and Pyle, 1988) comprising several lava flow sequences. Several lineaments have been mapped from landsat imageries in the region (Langston, 1981). Two sets of faults in NNE-SSW and NW-SE have been reported by several workers based on seismicity trends and focal mechanism solutions (Gupta, 1992; Talwani, 1997; Chadha et al. 1997; Rastogi et al., 1997; Rao and Shashidhar, 2016). Several ground cracks aligned in N-S direction were mapped by GSI (1968). Most of the regional structures inferred from geomorphology and tectonics, supported by geophysical data, suggest dominant N-S trending features (Talwani, 1997). Drilling in the NNE-SSW Donachiwada fault zone showed a 60° WNW dip of the fault (Gupta et al., 1999).

Our study delineates the local scale lineament fabric over the epicentral zone from airborne LiDAR survey and highlights its contribution in deciphering the seismicity pattern which is influenced by the annual cycles of water level changes in the reservoirs.

LINEAMENT FABRIC FROM AIRBORNE LiDAR

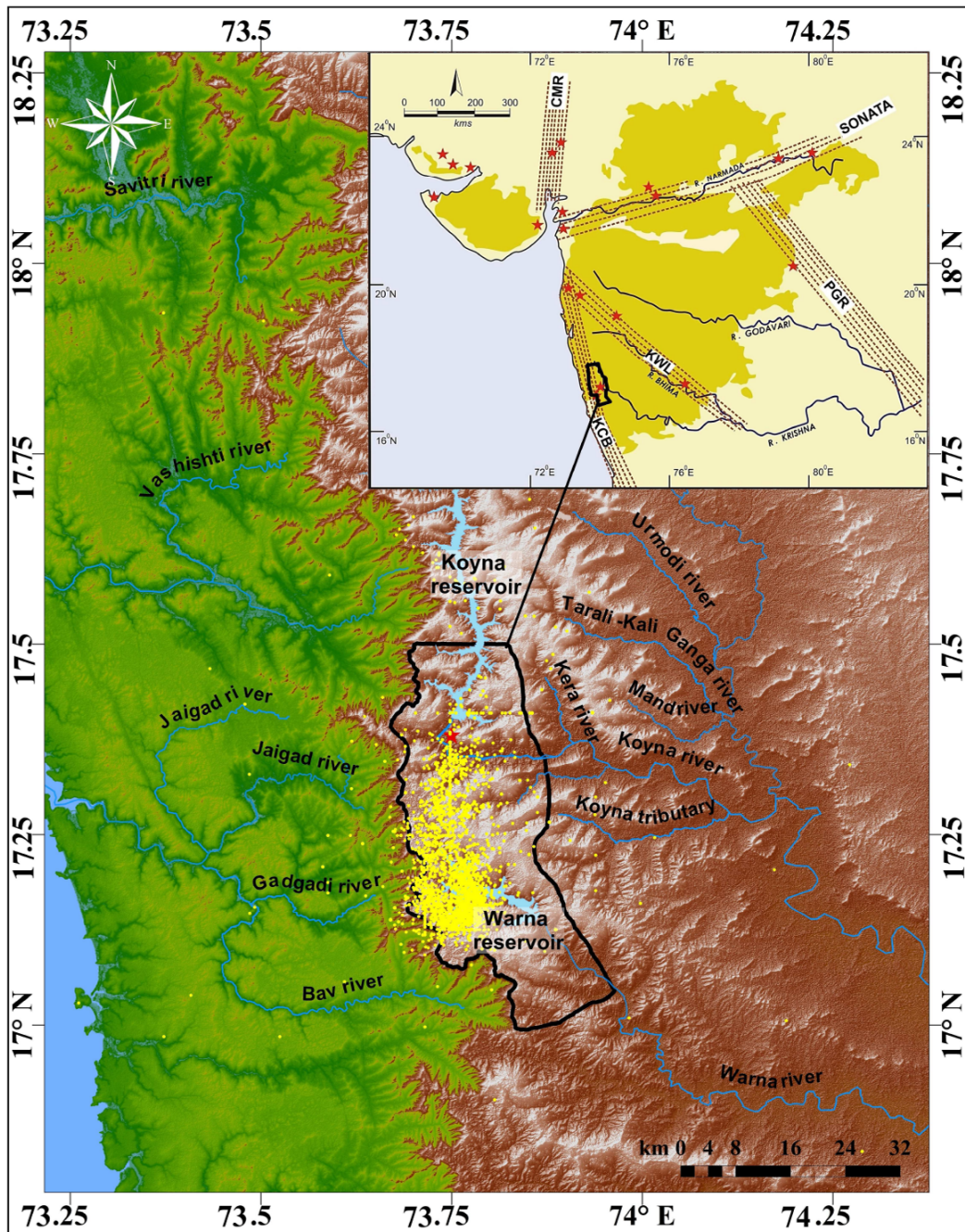
The high resolution airborne LiDAR (Light Detection and Ranging) is a powerful tool to map surface expressions of seismically active faults (Haugerud et al., 2003; Prentice et al., 2003). As the ground return of the LiDAR laser pulse can be separated from canopy returns, LiDAR data can be processed to virtually deforest the landscape and image the bare earth (Haugerud and Harding, 2001). Cunningham et al. (2006) used the technique to successfully map seismogenic faults in south eastern Alps of Slovenia. Hunter et al. (2011) identified strike-slip Polaris fault in north eastern California from LiDAR data and estimated deformation along it. Here we report the application of LiDAR mapping to image seismogenic faults that cut through forested mountainous terrain of the (KWSZ).

The LiDAR and orthophoto data was acquired on a Cessna 206 aircraft in the leaf-off month of April 2014 when vegetation cover is at its lowest so that penetration of the laser beam to the ground is maximised. The survey covered an area of 1064 sq km encompassing the seismically active Koyna-Warna Seismic Zone (KWSZ). Ground Control Points and Primary Survey Base were established about a month prior to the airborne survey. Sufficient GPS lock as well as quality monitoring of the IMU (Inertial Measurement Unit) was maintained to safeguard data quality. The average flight height was 650 m above ground, flight speed 90 knots/167 km per hour. Laser pulse of the Optech ORION M300 Airborne Laser Scanner was 125 kHz, scan frequency 71; Trimble 80 megapixel medium format aerial metric camera was used for the orthophoto capture with more than 60% overlap and distance between two photos as 205 m. With a point density of $6.09/m^2$ on the ground, the final vertical accuracy of LiDAR data in the area is 10 cm and horizontal accuracy is 15 cm; Orthomosaic Ground Sampling Distance (GSD) is 10 cm.

Figure 2 shows Bare Earth Model (BEM) from LiDAR data (Arora et al., 2017), which delineates lineaments showing persistence over tens of kilometres. Figure 2a highlights linear features aligned in NW-SE direction, the most prominent being the ridges to the north and south banks of the Warna reservoir. A NW-SE lineament extends from the northern tip of the Warna reservoir to the edge of the Western Ghar Escarpment (WGE). South of the Koyna reservoir, several sub-parallel NNW-SSE trends cut across the area including the E-W trending Koyna River. Figure 2b shows sub-parallel lineaments aligning mostly with the WGE. Figure 2c delineates the NE-SW features which are frequently manifested as alignments of subsidiary hills from north to south across the region.

SEISMICITY AND LINEAMENTS

A catalogue of $M \geq 4.0$ earthquakes was prepared for the Koyna-



Legend

- ★ Earthquake M 6.3 on Dec 10th 1967
 - KWSZ
 - ▭ LiDAR boundary area
 - River channel
- Ht(m)
1300
0

Fig. 1. The Koyna-Warna Seismic Zone (KWSZ) along Western Ghats Escarpment (WGE). Black outline shows airborne LiDAR survey coverage. Inset shows major tectonic feature along west coast and central India: CMR=Cambay Rift Zone, KCB=Konkan Coastal Belt, KWL=Kurduwadi Lineament, PGR=Pranhita Godavari Rift Zone, SONATA=Son Narmada Tapi belt, Red Stars=epicenters of M \geq 4.0 earthquakes.

Warna region for the period 1967 to 2016 for the present study. The catalogue is a compilation of data from CSIR-NGRI Seismological Observatory and CSIR-NGRI Koyna local digital network which became operational from 2005 onwards. Re-estimation of epicentral parameters by Gupta et al. (1980), Gupta (2002) and Talwani (1997) based on Maharashtra Engineering Research Institute (MERI) records are also included in the catalogue for completeness. During this period

more than two hundred M \geq 4.0 occurred; between 2013 and 2016 there were no earthquakes of M \geq 4.0. The last earthquake of M \geq 4.0 occurred in 2013.

Figure 3 shows epicenters of earthquakes in the Koyna-Warna region in the period 1968-2016. The earthquakes during 1967 are not taken into the analyses as they are dominated by aftershocks. The trend of the epicenters clearly defines a 10 km broad N-S dominated

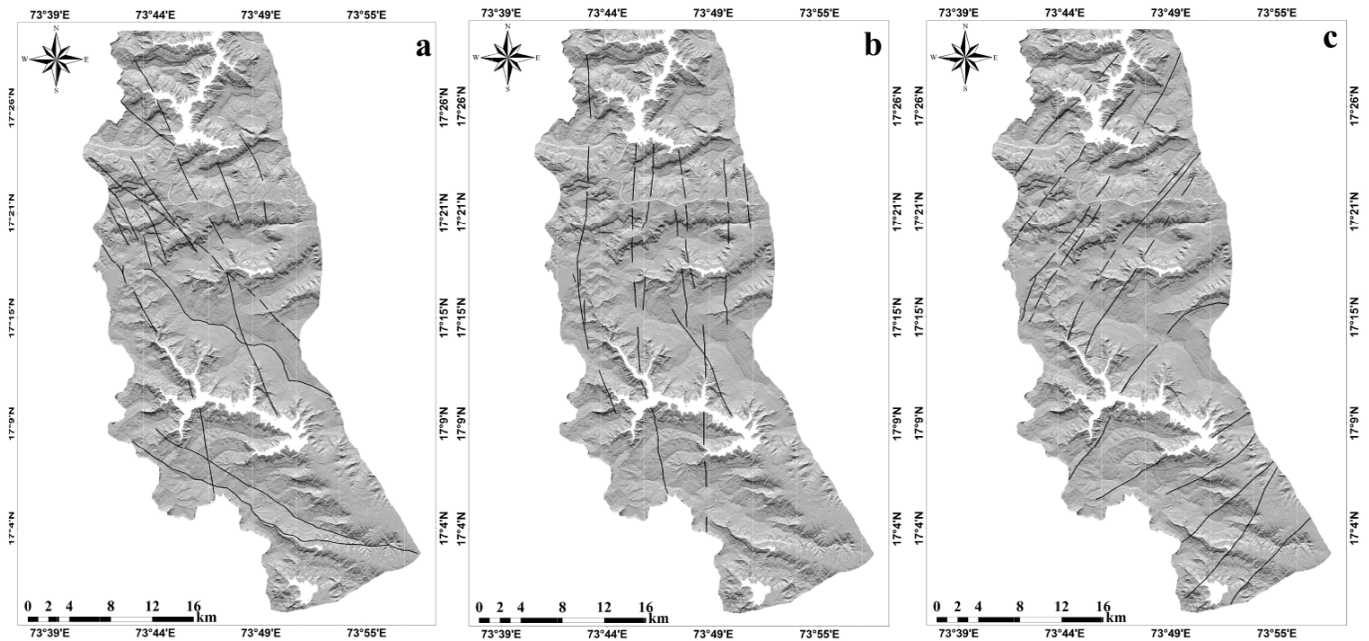


Fig.2. Lineaments delineated from LiDAR high resolution DEM in three directions (a) NW-SE, (b) N-S and (c) NE-SW.

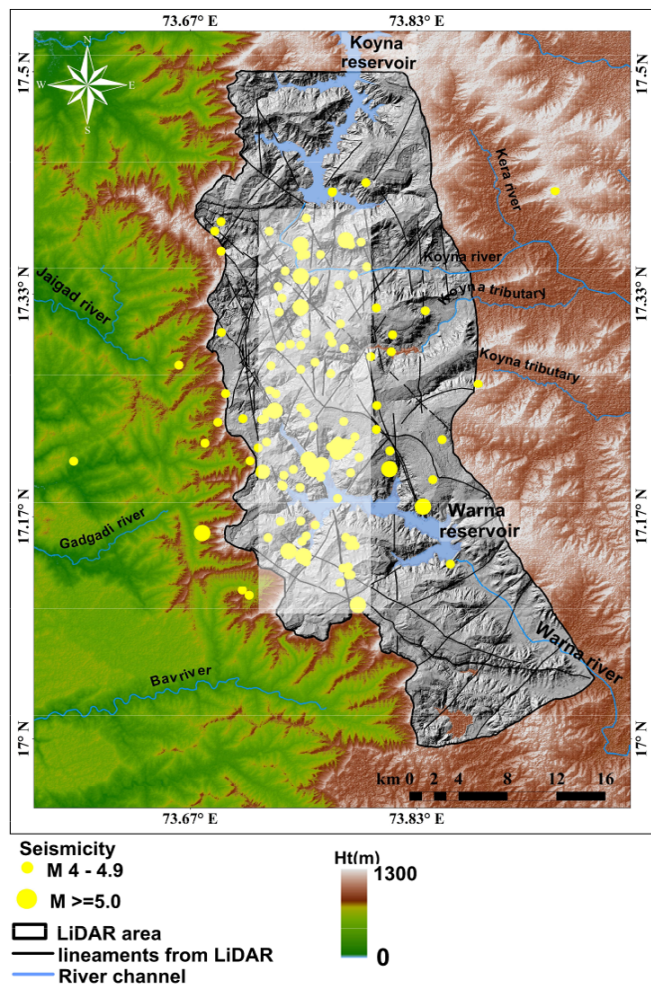


Fig.3. Epicentral distribution of $M \geq 4.0$ earthquakes for the period 1968-2016. A broad 10 km wide N-S zone is demarcated between Koyna and Warna reservoirs along which most of the earthquake occur. The zone shows LiDAR derived Digital Elevation Model (DEM) and lineaments in three directions but N-S fractures controls seismic activity.

lineaments zone between Koyna and Warna reservoirs which cut across several NW-SE and NE-SW lineaments in the area downstream of Koyna and upstream of Warna reservoirs along the WGE suggesting a strong structural control.

SEISMICITY AND HYDROGEOLOGICAL REGIME

The first recorded microearthquakes in the Koyna were reported soon after initial impounding of reservoir during 1961 monsoon and continued till the main of $M 6.3$ on December 10, 1967; they occurred mostly upstream of the Koyna dam (Gupta et al., 1980). After the main shock the seismic activity shifted southwards in a broad N-S zone by 25 km till the Warna River. The impounding of Warna reservoir in 1993 led to a burst of seismicity around the reservoir where it continues till today. Figure 4 shows month-wise distribution of $M \geq 4.0$ earthquakes for the period 1968 to 2016. Peaks in seismicity with $M \geq 4.0$ earthquakes were observed during September before the Warna reservoir was impounded. This pattern decayed after 1985 when a decrease in annual seismicity was observed. The impoundment of Warna reservoir in 1993 further enhanced triggered earthquakes upstream of Warna. Talwani (1997) made a similar observation based on reanalysis of earthquake data. Since then an additional peak in seismicity with earthquakes of $M \geq 4.0$ is observed during March-April, while the September activity continued and the December-January events reduced, indicating the role of altered hydrologic regime in the region. Earlier, Pandey and Chadha (2003) have shown that major episodes of earthquake energy release occur in two stages coinciding with annual filling and draining cycles of the Koyna reservoir. Smirnov et al. (2014, 2017) discussed the relationship of Koyna earthquakes with seismic parameters and reported seasonal patterns of seismicity.

The Koyna-Warna region gets an average of 88% of annual rainfall corresponding to 700-6000 mm during June-September affecting the hydrologic regime (Naik et al., 2003). The filling and draining cycles of both these reservoirs are a function of inflows during the rainfall and release of water for irrigation purposes. Figure 5 shows Warna reservoir volumes and Koyna reservoir volumes, annual inflows to reservoir, and discharge used to calculate infiltration. We calculated losses due to water percolation from the Koyna reservoir during the draining phase of the reservoir. The volume decreased during this

Table 1. Catalogue of $M \geq 4.0$ earthquakes from 1967 through 2016 compiled from various sources (Gupta, 1980, 2002; Talwani, Kumaraswamy and Sawalwade, 1996; NGRI Seismological Observatory, Hyderabad and NGRI Koyana local network, MERI, 2005). Total of 203 events are recorded, 123 of which have been located. For the current study, earthquakes located between 1968 and 2016 have been used.

S. No.	Year	Mon.	Date	Origin time	Mag	Depth (km)	Lat.	Long.
1	1967	9	13	6:23	5.8			
2	1967	9	13	6:47	4.5			
3	1967	9	13	6:51	4.0			
4	1967	9	13	7:01	4.0	5.00	17.348	73.787
5	1967	9	13	8:43	4.0			
6	1967	9	13	11:32	4.0			
7	1967	12	10	22:51	6.3	10.36	17.347	73.748
8	1967	12	11	20:49	5.4			
9	1967	12	12	18:20	4.7	15.00	17.234	73.757
10	1967	12	13	5:09	4.6	30.36	17.266	73.878
11	1967	12	13	19:19	4.6	27.94	17.411	73.935
12	1967	12	14	9:16	4.1	15.00	17.311	73.777
13	1967	12	14	15:06	4.1	6.19	17.287	73.799
14	1967	12	14	23:40	4.0	4.65	17.274	73.770
15	1967	12	22	14:48	4.8			
16	1967	12	24	3:41	4.0	26.8	17.277	73.748
17	1967	12	24	4:23	4.0	4.99	17.208	73.581
18	1967	12	24	23:49	5.0	15.00	17.202	73.813
19	1967	12	25	0:15	4.2	19.94	17.232	73.804
20	1967	12	25	0:47	4.2	15.00	17.248	73.748
21	1967	12	25	17:37	4.6	8.40	17.330	73.734
22	1967	12	25	17:59	4.1	5.08	17.293	73.780
23	1968	1	3	4:35	4.0	3.53	17.351	73.737
24	1968	1	11	4:37	4.1	0.63	17.409	73.771
25	1968	1	16	3:33	4.0	15.00	17.303	73.816
26	1968	2	7	8:09	4.3	8.23	17.294	73.733
27	1968	2	9	22:52	4.2	9.06	17.250	73.804
28	1968	2	12	9:13	4.5			
29	1968	3	4	21:36	4.3	6.19	17.2902	73.8145
30	1968	8	31	2:53	4.5	2.23	17.3873	73.6893
31	1968	9	20	10:11	4.4	5.76	17.4100	73.7713
32	1968	10	29	10:00	5.0	1.05	17.3700	73.7480
33	1968	10	30	11:29	4.1			
34	1968	11	23	11:12	4.1			
35	1969	1	21	22:32	4.1			
36	1969	2	13	18:26	4.2	8.04	17.3802	73.6847
37	1969	3	7	14:28	4.4	4.17	17.2797	73.7260
38	1969	6	3	23:26	4.2			
39	1969	6	27	20:05	4.5	3.53	17.3720	73.7923
40	1969	7	22	21:49	4.0			
41	1969	11	3	23:22	4.4	9.00	17.3202	73.7480
42	1969	11	4	5:11	4.2			
43	1970	4	16	14:46	4.0			
44	1970	5	27	12:45	4.8	3.52	17.3710	73.7480
45	1970	6	8	5:30	4.1			
46	1970	6	17	6:48	4.1			
47	1970	9	21	3:02	4.0			
48	1970	9	25	4:12	4.6	6.94	17.4172	73.7958
49	1970	9	26	16:36	4.6	7.12	17.2823	73.7585
50	1971	1	23	4:39	4.2			
51	1971	2	14	1:30	4.0	3.68	17.3402	73.7760
52	1971	8	10	4:30	4.0			
53	1971	8	10	6:15	4.3	13.63	17.2950	73.7480
54	1971	11	22	10:39	4.7	15.00	17.3802	73.7248
55	1972	5	1	21:11	4.2			
56	1972	5	11	11:49	4.5			
57	1972	7	5	23:17	4.0			
58	1972	11	11	4:02	4.1			
59	1973	4	19	8:45	4.1			
60	1973	10	17	8:03	4.0			
61	1973	10	17	14:13	4.1	5.00	17.3900	73.7520
62	1973	10	17	15:24	5.0	4.05	17.3735	73.7812
63	1974	2	17	14:06	4.5	8.02	17.1632	73.7480
64	1974	4	28	9:30	4.0			

Table 1 Contd....

S. No.	Year	Mon.	Date	Origin time	Mag	Depth (km)	Lat.	Long.
65	1974	5	29	18:26	4.2			
66	1974	7	29	23:17	4.8	19.01	17.3208	73.8395
67	1974	8	7	4:23	4.1			
68	1974	8	28	20:20	4.5	5.03	17.2072	73.7517
69	1974	11	11	15:11	4.3	5.96	17.2260	73.7878
70	1974	12	20	14:16	4.0	5.00	17.3628	73.7517
71	1975	2	10	18:35	4.0	5.00	17.3537	73.7965
72	1975	9	2	23:17	4.2	5.97	17.3390	73.7313
73	1975	12	2	7:40	4.2	0.13	17.2368	73.6870
74	1975	12	24	13:25	4.3	6.87	17.2213	73.6775
75	1976	3	14	5:16	4.8	3.98	17.2438	73.7517
76	1976	4	22	10:46	4.3	0.03	17.2802	73.6583
77	1976	9	16	14:04	4.2			
78	1976	9	26	6:48	4.3			
79	1976	12	12	0:52	4.2	5.00	17.3040	73.7517
80	1977	9	19	0:03	4.7	5.56	17.3230	73.8035
81	1977	11	4	18:56	4.0			
82	1977	11	4	20:36	4.2			
83	1977	11	4	20:55	4.4			
84	1978	11	29	5:30	4.0			
85	1978	12	12	15:01	4.4	5.47	17.2210	73.7845
86	1979	1	26	19:12	4.0			
87	1979	9	26	20:02	4.0			
88	1980	2	6	22:13	4.6	6.82	17.1508	73.7238
89	1980	8	19	22:32	4.2			
90	1980	9	2	16:39	5.3	14.02	17.1740	73.8378
91	1980	9	2	16:47	4.5			
92	1980	9	20	7:28	5.5	15.00	17.1408	73.7390
93	1980	9	20	10:45	5.8	15.00	17.1543	73.6755
94	1980	9	20	11:22	4.5			
95	1980	9	20	14:27	4.0			
96	1980	9	20	23:44	4.2			
97	1980	9	21	0:00	4.0			
98	1980	9	21	3:52	4.0			
99	1980	9	21	18:19	4.0			
100	1980	9	22	11:59	4.3			
101	1980	9	25	13:38	4.3			
102	1980	9	27	8:54	4.0			
103	1980	9	30	13:37	4.2			
104	1980	10	3	15:20	4.4			
105	1980	10	4	16:37	5.1	5.52	17.2020	73.7575
106	1980	10	4	19:10	4.3			
107	1980	10	5	16:10	4.0			
108	1980	10	16	21:26	4.1			
109	1980	10	17	21:47	4.1			
110	1980	10	21	5:02	4.2			
111	1980	10	26	1:32	4.5			
112	1981	1	25	20:30	4.0			
113	1982	4	25	23:04	4.4	7.09	17.2017	73.7425
114	1982	5	5	7:32	4.2	5.01	17.2395	73.7212
115	1982	9	10	2:42	4.4			
116	1983	2	5	22:52	4.3	2.18	17.3047	73.6897
117	1983	3	21	15:02	4.1	6.53	17.2185	73.7698
118	1983	5	13	5:53	4.1	6.22	17.2612	73.7252
119	1983	5	28	18:08	4.2	21.77	17.2958	73.7403
120	1983	9	25	18:55	4.8	0.51	17.2240	73.8518
121	1983	11	10	8:55	4.5			
122	1984	9	25	7:47	4.6	15.00	17.5470	73.7852
123	1984	11	14	11:58	4.7	8.20	17.2375	73.7795
124	1984	12	21	17:26	4.1	8.69	17.2228	73.7755
125	1985	5	27	6:57	4.1	9.51	17.2397	73.7055
126	1985	10	29	8:33	4.0			
127	1985	10	29	13:59	4.2			
128	1985	11	15	7:02	4.3			
129	1985	11	21	9:28	4.0			
130	1985	11	21	11:39	4.1			
131	1985	12	15	13:11	4.3	7.36	17.3627	73.7625
132	1985	12	28	14:52	4.0	20.45	17.3618	73.7480
133	1988	7	24	5:33	4.8	15.00	17.1992	73.7847

Table 1 Contd....

S. No.	Year	Mon.	Date	Origin time	Mag	Depth (km)	Lat.	Long.
134	1988	8	15	22:16	4.0	7.30	17.2582	73.7297
135	1988	8	15	23:27	4.1	9.29	17.3652	73.6893
136	1988	9	11	20:39	4.4	12.68	17.2155	73.8135
137	1989	10	29	7:30	4.0	7.10	17.3700	73.7847
138	1990	7	3	13:28	4.1			
139	1991	1	6	22:13	4.4	6.27	17.1973	73.7355
140	1992	2	20	5:42	4.3	7.59	17.2583	73.6927
141	1992	4	1	1:34	4.0	5.77	17.3198	73.7322
142	1993	8	27	22:12	4.1	2.41	17.2147	73.7775
143	1993	8	28	4:27	5.3	11.92	17.2187	73.7798
144	1993	8	28	8:31	4.0	15.00	17.2107	73.7908
145	1993	9	3	23:03	5.0	13.75	17.2090	73.7537
146	1993	9	4	0:53	4.3	1.23	17.1958	73.7627
147	1993	10	22	1:15	4.1	11.01	17.1327	73.7518
148	1993	10	22	15:35	4.1			
149	1993	12	8	1:42	5.2	8.23	17.2050	73.7632
150	1993	12	21	10:10	4.1	12.15	17.1603	73.7587
151	1994	1	22	11:12	4.0	8.11	17.1882	73.7475
152	1994	2	1	9:31	5.5	8.83	17.3235	73.7480
153	1994	3	29	7:51	4.3	6.55	17.2080	73.7107
154	1994	10	31	6:10	4.2	9.93	17.2182	73.7735
155	1995	3	12	8:22	5.1	7.54	17.2457	73.7288
156	1995	3	13	3:09	4.9	5.37	17.2222	73.7228
157	1995	3	20	6:58	4.1	5.22	17.2390	73.7193
158	1995	4	15	22:59	4.2	8.49	17.2178	73.7167
159	1995	9	5	0:54	4.0			
160	1995	11	8	20:06	4.1			
161	1995	11	15	4:08	4.1			
162	1996	4	26	12:19	4.6			
163	1996	4	26	12:36	4.2			
164	1997	4	25	16:22	4.3	5.00	17.3430	73.7580
165	1998	2	11	1:08	4.7			
166	1998	2	14	0:59	4.4			
167	1999	6	7	15:45	4.3	3.00	17.3020	73.7690
168	2000	3	12	18:03	5.6	15	17.2000	73.7200
169	2000	3	13	20:46	4.0			
170	2000	4	6	22:30	5.1	8.00	17.1370	73.7500
171	2000	4	27	23:21	4.1	5.00	17.1630	73.7330
172	2000	9	5	0:32	5.6	10.00	17.2150	73.7750
173	2000	12	8	13:23	4.1	5.00	17.1480	73.7490
174	2001	3	19	16:38	4.0	8.00	17.1900	73.7340
175	2001	5	17	16:04	4.4	8.00	17.1890	73.7350
176	2001	8	2	4:09	4.2			
177	2003	3	22	1:00	4.0			
178	2003	3	27	6:18	4.2			
179	2005	3	14	9:43	5.2	13	17.1000	73.7900
180	2005	3	15	2:07	4.2			
181	2005	3	26	0:56	4.1			
182	2005	6	7	21:32	4.3			
183	2005	6	15	2:19	4.1			
184	2005	8	14	6:33	4.2	15.00	17.1310	73.8580
185	2005	8	30	8:53	4.8	15.00	17.1940	73.8450
186	2005	11	13	3:56	4.2	6.70	17.1510	73.7810
187	2005	11	20	18:50	4.0	6.50	17.2210	73.7730
188	2005	12	26	10:46	4.2	4.80	17.1490	73.7860
189	2006	4	17	16:40	4.6	4.20	17.1450	73.7850
190	2007	8	20	19:16	4.2	5.10	17.1450	73.7840
191	2007	11	24	10:57	4.5	5.80	17.1110	73.7050
192	2007	11	24	11:35	4.2	5.50	17.1070	73.7100
193	2008	7	29	19:11	4.0	13.5	17.3240	73.7470
194	2008	9	16	21:47	4.7	9.00	17.2970	73.7710
195	2009	11	14	13:34	4.7	3.90	17.1170	73.7770
196	2009	12	12	11:51	4.1	4.70	17.1290	73.7830
197	2009	12	12	21:56	4.8	1.50	17.1450	73.7880
198	2009	12	23	3:49	4.1	4.10	17.1230	73.7830
199	2010	1	12	9:25	4.0	4.30	17.1230	73.7850
200	2010	5	24	8:00	4.0	4.00	17.1280	73.7790
201	2012	4	14	5:27	4.6	8.00	17.3240	73.7450
202	2013	1	26	2:24	4.1	7.20	17.1520	73.7520
203	2013	9	5	16:40	4.0	5.90	17.2440	73.7230

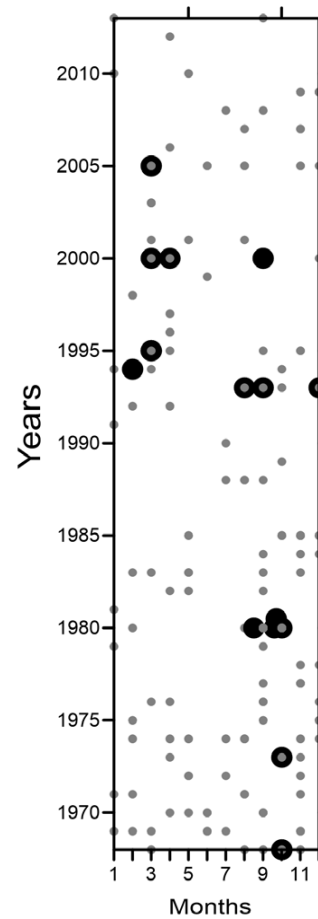


Fig.4. Month-wise distribution of $M \geq 4.0$ earthquakes over the years 1968-2016. Grey dots represent earthquakes of $4.0 \leq M < 4.9$; black circles represent earthquakes of $M \geq 5.0$. Major episodes of seismic activity with $M \geq 4.0$ earthquakes are seen during loading period of Koyna reservoir during 1968 to 1985. A decrease in annual occurrence of seismicity is seen during 1986 to 1992. Another episode of seismic activation is observed after Warna reservoir impoundment from 1993 onwards during March-April in addition to September.

phase, ΔV results from the Dam releases (R_D), the evaporation (ET) and the infiltration (I), as available in the Koyna dam database. Using the following equation,

$$\Delta V = R_D + ET + I$$

where $\Delta V < 0$ during the draining phase, the infiltration can be calculated as follows,

$$I = \Delta V - (R_D - ET)$$

During the filling phase the volume variation results from the input of the precipitation (P) and the output seen above. Thus, the infiltration can be determined following these equations:

$$\Delta V = P - (R_D + ET + I)$$

$$I = P - \Delta V - R_D - ET$$

Figure 6 shows month-wise Warna and Koyna volumes, averaged over the years since the impoundment of each reservoir, as well as infiltration from Koyna reservoir. It is seen that infiltration starts immediately after the Koyna reservoir receive initial inflows from rainfall in June and peak during July even before the reservoir attains its maximum level. Infiltration remains constant during July-September when the reservoir reaches its maxima. Infiltration starts declining when the reservoir volume starts decreasing when the water from the

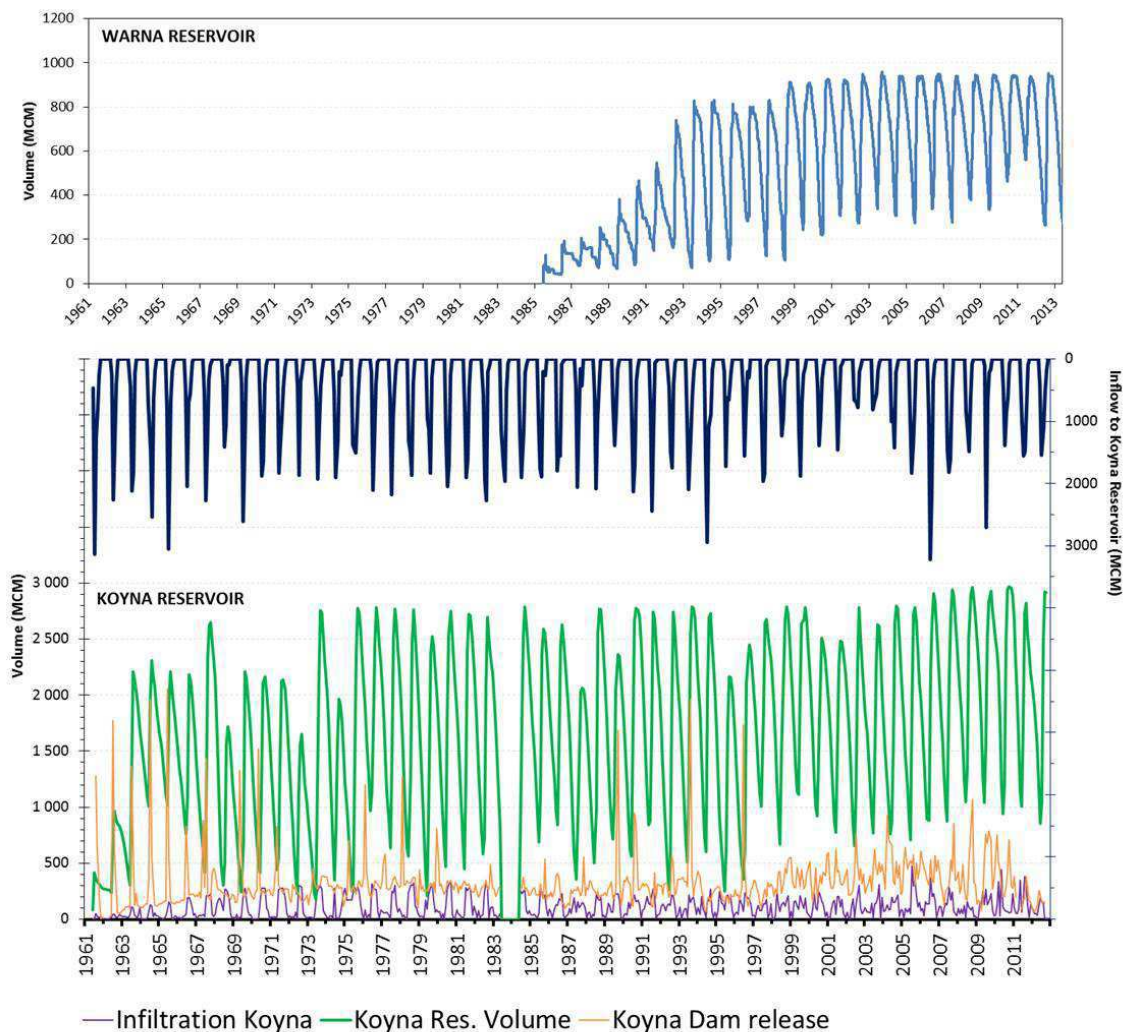


Fig.5. Warna reservoir volume in top panel and Koyna reservoir water balance in bottom panel: Inflow into the reservoir over Koyna watershed (900 km²) in blue, Koyna reservoir volume in green, release from the Koyna Dam in orange and calculated losses by infiltration in purple.

reservoir is released for irrigation purpose from October onwards. An average infiltration of 95 MCM per month was obtained for the studied period for Koyna reservoir which is about 5% of the reservoir volume. Considering the volume difference between the two reservoirs, i.e., about 1900 MCM for Koyna and 540 for Warna, the infiltration from Warna is considered to be much less. Peaks in seismicity in September and December are observed during 1968 to 1993 prior to the impounding of Warna reservoir. Post Warna impounding 1993 onwards, the seismicity peak is observed during March-April with diminished peaks in September and December indicating a clear change in the effect of the change in hydro-geological environment on earthquake occurrence.

DISCUSSION

Over the past five decades triggered earthquakes continue to occur in the Koyna Warna Seismic Zone in western India. To decipher the fault system(s) along which the seismicity is occurring, airborne LiDAR mapping was done to find surface expression of these seismically active faults. We prepared a catalogue of $M \geq 4.0$ earthquakes in the Koyna-Warna region for the period 1967 to 2016 and critically analysed five decades of data to understand the seismotectonics and hydro-geological regime in the region. The earthquakes in the region are found to occur downstream of the Koyna and upstream of the Warna reservoirs in a prominent N-S zone of about 10 km width. The latter is a deviation from most of the Reservoir Triggered Seismicity (RTS) cases where earthquakes are generally found to occur downstream of a reservoir

leading to the inference that seismic activity in the Koyna-Warna region is strongly controlled by the N-S structural zone. The presence of the N-S fault zone is supported by evidences like alignment of hot springs along the N-S Western Ghats Escarpment which itself is believed to be faulted (Pascoe, 1964; Valdiya, 1984).

We report changes in the seismicity pattern and relate it to hydro-geological regime changes over a period of time which modified local stresses in the region. Percolation of water along pre-existing faults close to critical tectonic stress can trigger slip by increasing pore pressures through diffusion process (Castle et al., 1980). The initial impounding of Koyna reservoir, which began in 1961 initiated micro-earthquake activity with $M \leq 3.0$ events starting in 1963 indicating that the stresses were already near critical failure. Prior to this activity, the region had experienced only two felt earthquakes (Verma, 1985). Annual cyclic variations in the Koyna reservoir levels from 1968 to 2013 showed persistent earthquake peaks during loading cycle in September and a delayed effect in December with few events as background seismicity throughout the year. The impounding of Warna reservoir in 1993 initiated intense seismic activity around the reservoir with peak during March-April in addition to September and a decreased activity in December.

Figure 7 shows a cartoon depicting the association of seismicity vis-à-vis hydro-geological regime which was altered after the impounding of the Warna reservoir. We hypothesise that during pre-Warna the infiltration from Koyna reservoir was primarily controlled by the geometry of fracture network along the N-S zone delineated by

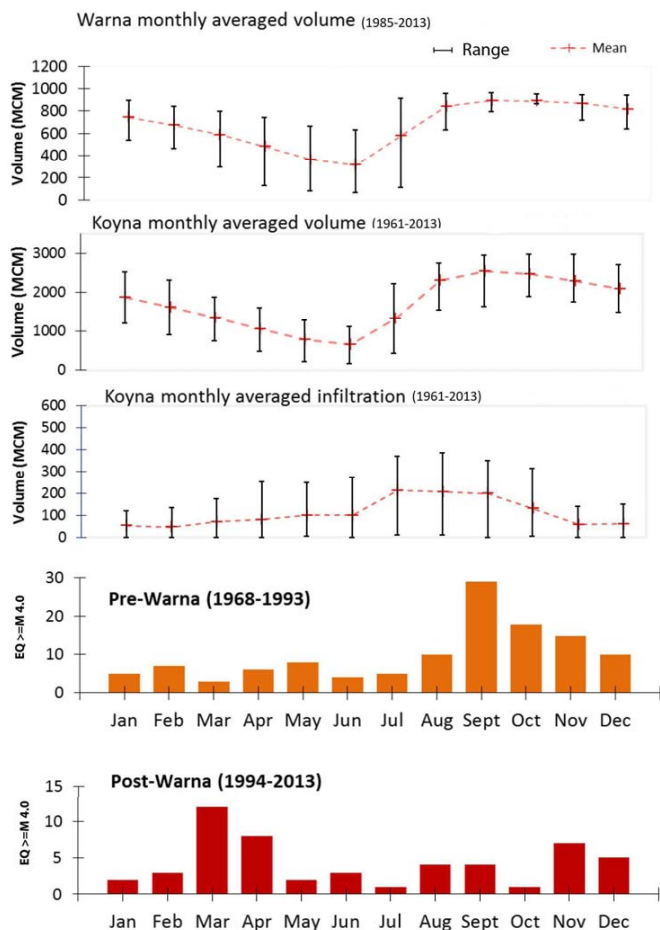


Fig.6. Monthly averages of the Warna and Koyna reservoir volumes over the years since their respective impoundment and monthly averages of the infiltration volume of the Koyna reservoir. Monthly distribution of earthquakes (for $M \geq 4.0$) during pre Warna (orange) shows prominent peak during September, which declining trend till December and during post Warna (brown) March-April peak becomes prominent with diminished peaks in September and December.

LiDAR, creating pore pressure build up south of the Koyna reservoir, in near and far field, triggering earthquakes during the filling cycle in September. The movement of pore pressure front aided by continued, though diminished infiltration during the draining cycle, further triggers earthquakes in December as delayed effect. The earthquakes are observed south of Koyna to distances up to 25 km till the Warna River and are mostly deeper, 5-15 km (Table 1). Post Warna, a changed scenario was created where additional infiltration, although of small volumes, began from the Warna reservoir into the N-S fracture network and resulted in a burst of seismicity after it attained its full capacity in 1993. While the seismicity pattern with peak in September continued with decreased frequency, under the combined impact of Koyna and Warna reservoirs a new peak was observed in March-April with most of the earthquakes becoming shallower, <10km (Table 1). Dixit et al. (2014) also indicated a shallower water saturated crust around the Warna reservoir, based on local network tomography. The westward dipping faults (Gupta et al., 1999) and associated fracture zones, along with the westward drop of ~100 m (over 15 km) of basement topography from the plateau area to the Konkan coastal plains (as inferred from borehole basement depths Gupta et al. (2016)) explains the concentration of seismicity in the western portion of the plateau area, including the area near the Warna reservoir. The present day seismic activity is mostly confined to Warna reservoir with few earthquakes occurring downstream of Koyna.

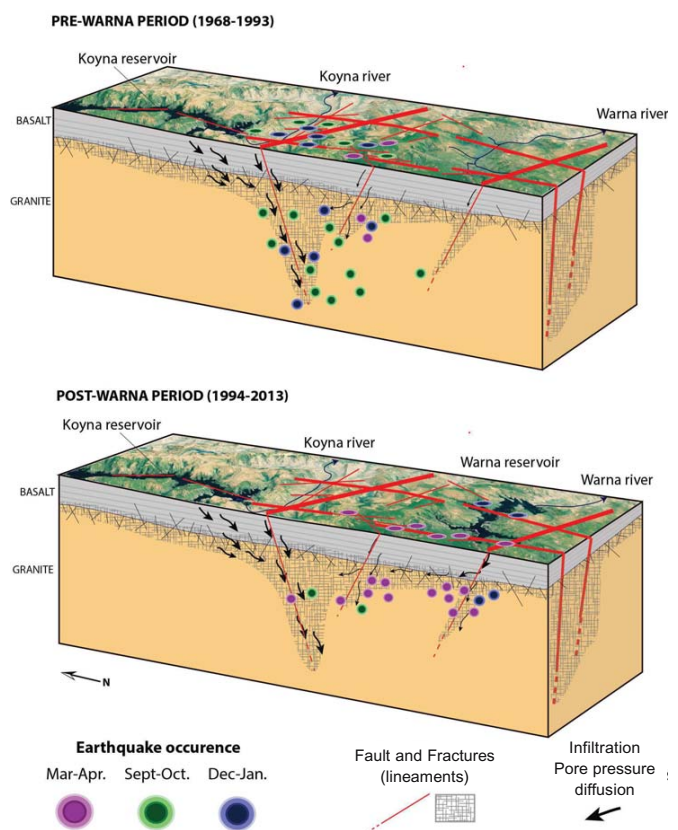


Fig.7. A cartoon showing the conceptual model to explain the seismic activity along the main N-S fault system and fracture zone and the impact of Warna reservoir impounding in changing hydro-geological regime and shift in seismicity.

CONCLUSIONS

1. The epicentral distribution of $M \geq 4.0$ earthquakes during 1968-2013 show a dominant trend along a 10 km broad N-S zone between Koyna and Warna reservoirs delineated by airborne LiDAR mapping. The dense fracture fabric in this zone plays a crucial role in linking hydro-geological regime to the genesis of triggered earthquakes.
2. Seismicity peaks prior to impoundment of Warna reservoir are observed during September and December related to pore pressure diffusion process south of Koyna reservoir.
3. Intense seismicity was triggered upstream of Warna reservoir post impounding in 1993. Annual cycles of reservoir loading indicate additional peak seismicity during March-April caused by changes in the hydro-geological regime in the region.

Acknowledgements: The authors are thankful to the Ministry of Earth Sciences, Government of India for providing funds for LiDAR survey, Director, CSIR-National Geophysical Research Institute for support. We are indebted to Prof. Harsh Gupta, the Editor, for guidance with the seismological data and valuable suggestions for the improvement of the manuscript. Colleagues from Seismological Observatory, CSIR-NGRI are gratefully acknowledged for help in constructing the catalogue. A part of the work is supported by a joint DST (Project No. INT/RUS/RSF/p-13) RSF project No.16-47-02003.

References

- Arora, K., Y. Srinu, Selles, A. and Chadha, R.K. (2017) Airborne LiDAR mapping of active faults in the Koyna-Warna Seismic zone, Western India: implications for triggered earthquake. communicated to JGR, Solid Earth.
- Castle, R.O., Clark, M.M., Grantz, A., Savage, J.C. (1980) Tectonic state: its

- significance and characterization in the assessment of seismic effects associated with reservoir impounding. *Engg. Geol.*, v.15, pp.53–103.
- Cunningham, D., Grebby, S., Tansey, K., Gosar, A., and Kastelic, V. (2006) Application of airborne LiDAR to mapping seismogenic faults in forested mountainous terrain, southeastern Alps, Slovenia; *Geophys. Res. Lett.*, v.33, L20308, doi:10.1029/2006GL027014.
- Chadha, R.K., Gupta, H.K., Kuempel, H.J., Mandal, P., Nageswara Rao, A., Narendra Kumar, Radhakrishna, I., Rastogi, B.K., Raju, I.P., Sarma, C.S.P., Satyamurthy, C. and Satyanarayana, H.V.S. (1997) Delineation of active faults, nucleation process and pore pressure measurements at Koyna (India). *Pure. Appld. Geophys.*, v.150, no.3/4, pp.551-562.
- Dixit M.M., Kumar S., Catchings R.D., Suman K., Sarkar D., Sen M.K. (2014) Seismicity, faulting and structure of the Koyna-Warna seismic region, Western India from local earthquake tomography and hypocenter locations. *Jour. Geophys. Res.*, v.119, pp.6372-6398.
- Duncan, R.A. and Pyle, D.G. (1988) Rapid eruption of Deccan flood basalts at the Cretaceous/Tertiary boundary., *Nature*, v.333, pp.841–843.
- Geological Survey of India (1968) A Geological Report on the Koyna Earthquake of 11th December, 1967. Satara District, Maharashtra State, India.
- Gupta, H.K., Rao, C.V.R and Rastogi, B.K. (1980) An investigation of earthquakes in Koyna region, Maharashtra, for the period October 1973 through December 1976. *Bull. Seismol. Soc. Amer.*, v.70, pp.1833–1847.
- Gupta, H.K. (1992) *Reservoir Induced Earthquakes*. Elsevier, Amsterdam, 364p.
- Gupta, H.K., Rao, R.U.M., Srinivasan, R., Rao, G.V., Reddy, G. K., Dwivedy, K.K., Banerjee, D.C., Mohanty, R., Satyasradhi, Y.R. (1999) Anatomy of surface rupture zones of two stable continental region earthquakes, 1967 Koyna and 1993 Latur, India. *Geophys. Res. Lett.*, v.26, no.13, pp.1985–1988.
- Gupta, H.K. (2002) A review of recent studies of triggered earthquakes by artificial water reservoirs with special emphasis on earthquakes in Koyna, India. *Earth Sci. Rev.*, v.58, pp.279–310.
- Gupta, H.K. (2005) Artificial water reservoirs-triggered earthquakes with special emphasis at Koyna. *Curr. Sci.*, v.88, no.10, pp.1628-1631.
- Gupta, H.K., Kusumita Arora, Rao, N.P., Sukanta Roy, Tiwari, V.M., Prasanta K. Patro, Satyanarayana, H.V.S., Shashidhar, D., Mahato, C.R., Srinivas, K.N.S.S.S., Srihari, M., Satyavani, N., Srinu, Y., Gopinath, D., Haris Raza, Monikuntala Jana, Vyasulu V. Akkiraju, Deepjyoti Goswami, Digant Vyas, Dubey, C.P., Raju, D.Ch.V., Ujjal Borah, Kashi Raju, Chinna Reddy, K., Narendra Babu, Bansal, B.K. Shailesh Nayak (2016) Investigations of continued reservoir triggered seismicity at Koyna, India. *Geol. Soc. London, Spec. Publ*, v.445, pp.151-188.
- Haugerud, R.A. and Harding, D.J. (2001) Some algorithms for virtual deforestation (VDF) of Lidar topographic survey data., *Int. Arch. Photogramm, Remote Sens.*, v.XXXIV-3/W4, pp.211–217.
- Haugerud, R.A., Harding, D.J., Johnson, S.Y., Harless, J.L., Weaver, C.S. and Sherrod, B.L. (2003) High-resolution Lidar topography of the Puget Lowland, Washington—A bonanza for Earth science. *GSA Today*, v.13, pp.4–10.
- Hunter, L.E., Howle, J.F., Rose, R.S. and Bawden, G.W. (2011) LiDAR-Assisted Identification of an Active Fault near Truckee, California. *Bull. Seismol. Soc. Amer.*, v.101, no.3, pp.1162–1181.
- Langston, C.A. (1981) Source inversion of seismic waveforms: the Koyna, India, earthquakes of 13 September 1967. *Bull. Seismol. Soc. Amer.*, v.71, pp.1–24.
- Naik, P.K. and Awasthi, A.K. (2003) Groundwater resources assessment of the Koyna River basin, India. *Hydrogeol. Jour.* v.11(5), pp.582–94.
- Pandey, A.P. and Chadha, R.K. (2003) Surface loading and triggered earthquakes in the Koyna-Warna region, western India. *Phys. Earth Planet. Inter.*, v.139, pp.207-223.
- Pascoe, E.H. (1964) *A Manual of the Geology of India and Burma*, vol. 3. Government of India Press, Calcutta.
- Prentice, C.S., Crosby, C.J., Harding, D.J., Haugerud, R.A., Merritts, D.J., Gardner, T.W., and Baldwin, J.N. (2003) Northern California LIDAR Data: A Tool for Mapping the San Andreas Fault and Pleistocene Marine Terraces in Heavily Vegetated Terrain; American Geophysical Union, Fall Meeting 2003, abstract #G12A-06.
- Rao, N.P. and Shashidhar, D. (2016) Periodic variation of stress field in the Koyna–Warna reservoir triggered seismic zone inferred from focal mechanism studies. *Tectonophysics*, v.679, pp.29–40.
- Rastogi, B.K., Chadha, R.K., Sarma, C.S.P., Mandal, P., Satyanarayana, H.V.S., Raju, I.P., Narendra Kumar, Satyamurthy, C. and Nageswara Rao, A. (1997) Seismicity at Warna Reservoir (near Koyna) through 1995. *Bull. Seismol. Soc. Amer.*, v.87, pp.1487-1494.
- Scholz, H. (2002) *The mechanics of earthquakes and faulting*. Cambridge Univ. Press, pp.471.
- Smirnov, V., Chadha, R.K., Ponomarev, A., Srinagesh, D., Potanina, M. (2014) Triggered and tectonic driven earthquakes in the Koyna–Warna region, western India. *Jour. Seismol.*, v.18, pp.587–603. DOI: 10.1007/s10950-014-9430-7
- Smirnov, V., Srinagesh, D., Ponomarev, A.V., Chadha, R.K. and Mikhailov, V.O., Potanina, M.G., Kartashov, I.M. and Stronganova, S.M. (2017) The behavior of seasonal variations in induced seismicity in the Koyna–Warna region, western India, *Izvestia, Phys.Solid.Earth.*, v.53, no.4, pp.530-539.
- Talwani, P. (1997) *Seismotectonics of the Koyna-Warna area, India*. Pure. Appld. Geophys., v.150, pp.511–550.
- Talwani, P., Kumaraswamy, S.V. and Sawalwade, C.B. (1996) Re-analysis of earthquakes of Koyna-Warna, 1963-1995, MERI Report.
- Valdiya, K.S. (1984) *Aspects of Tectonics: Focus on South-Central Asia*. McGraw-Hills, New Delhi.
- Verma, R.K. (1985) *Gravity field, Seismicity and Tectonics of the Indian Peninsula and the Himalayas*. D. Reidel Publishing Company, Boston, 213p.